Hindawi Publishing Corporation
Shock and Vibration
Volume 2015, Article ID 478045, 9 pages
http://dx.doi.org/10.1155/2015/478045

Research Article

Investigation of ΔE Effect on Vibrational Behavior of Giant Magnetostrictive Transducers

M. Sheykholeslami,[1] Y. Hojjat,[1] M. Ghodsi,[2] K. Kakavand,[1] and S. Cinquemani[3]

[1]*Faculty of Engineering, Tarbiat Modares University, Jalale-Ale-Ahmad Highway, P.O. Box 14115/143, Tehran, Iran*
[2]*College of Engineering, Sultan Qaboos University, P.O. Box 33, Al-Khod, 123 Muscat, Oman*
[3]*Department of Mechanics, Politecnico di Milano, Via La Masa 1, 20156 Milano, Italy*

Correspondence should be addressed to Y. Hojjat; yhojjat@modares.ac.ir

Received 19 November 2014; Accepted 26 January 2015

Academic Editor: Alicia Gonzalez-Buelga

Resonant magnetostrictive transducers are used for generating vibrations in the sonic and ultrasonic range of frequency. As the mechanical properties of magnetostrictive materials change according to different operating conditions (i.e., temperature, mechanical prestress, and magnetic bias), the vibrational behavior of the transducer changes too. ΔE effect is the change in the Young modulus of the ferromagnetic material and it has to be considered as it leads to changes in the dynamics of the transducer. This paper deals with the study of such effect from both theoretical and experimental point of view. ΔE effect on behavior of the transducer based on Terfenol-D is analytically described as a function of different operating conditions focusing on effects on resonance frequency, mode shape, and moreover experimentally the quality factor. Results of resonance frequency prediction have been validated with experiments and good agreement has been seen.

1. Introduction

Magnetostrictive materials exhibit some interesting properties such as the ability to change their shape when a magnetic field varies along the material itself (Joule effect) [1–4]. This effect has been exploited to realize transducers devoted to generate vibration from low range of frequency to sonic and ultrasonic range of frequency. While low frequency range is commonly used in active vibration control applications [5–7] sound [8], sonic, and ultrasonic transducers are used as sonar transducers [9, 10], machining transducers [11] and so forth.

Despite benefits in using magnetostrictive materials in transducers, mechanical properties of the material, such as Young modulus, change according to the operational condition such as prestress, magnetic bias, and temperature. This phenomenon is called ΔE effect. Among ferromagnetic material, ΔE effect in Terfenol-D has the highest value [12]. Study on the ΔE effect in Terfenol-D and related considerations has been presented in different papers [13–15], but some disagreements about results can be observed, probably due to interferences of various parameters in Young modulus measurement. Some other works have been tried to use ΔE effect in Terfenol-D devices in passive operation such as tunable resonator [16]. Some efforts have been done to use this effect for modeling and optimizing nonresonant Terfenol-D actuator. Yong and Lin [17] presented a dynamic model for giant magnetostrictive actuator considering ΔE effect, while Ueno et al. [18] introduced magnetic design circuit method for magnetic force control system with considering ΔE effect for the Terfenol-D to improve the efficiency of the device. Dapino et al. [19] introduced a model for ΔE effect in the magnetostrictive transducer. In this model, there is a discussion about ΔE in resonance frequency of the transducer. Changing resonance frequency in this transducer was 140 Hz for sweeping magnetic bias from the first region of application to saturated region.

Notwithstanding these works, there is no report about consequences of ΔE effect on operational parameters of Terfenol-D resonant transducers. As a matter of fact, resonance frequency, mode shape, and mechanical quality factor of the transducer depend on the Young modulus of the magnetostrictive material. When resonance frequency is changed, due to ΔE effect, the transducer starts working in nonresonance region, thus decreasing its performance. For this reason, it is important to predict the effect of these changes due to a change in the Young modulus of the material, to adjust the functioning of the transducer accordingly.

To achieve these goals, a resonant Terfenol-D transducer has been designed and fabricated. Main parameters causing ΔE effect are measured to experimentally to find out their correlation with the change of the Terfenol-D Young modulus. Vibrational behavior of the transducer is modeled analytically and numerically using ANSYS12 commercial software. Predictions results have been satisfactorily verified with experiments. Results can be helpful in using the Terfenol-D transducer in order to permanently adjust it in resonance region during operation. Also effect of changing condition on performance of the transducer can be predictable based on these results.

The paper is structured as follows. Section 2 introduces an analytical model to take into account the effect of main mechanical parameters of a resonant transducer and its operating conditions on the resonance frequency, mode shape, and the quality factor of the device. Section 3 presents the transducer used to validate the model and the experimental set-up. Section 4 collects results from both analytical and experimental analysis. A discussion of results is done and conclusions are drawn in Section 5.

2. ΔE Effect in Resonant Transducers

Resonant Langevin transducers are used to generate sonic and ultrasonic vibration. As suggested in their name, these devices should work in resonance frequency to enhance mechanical vibration. These devices are characterized by a very narrow bandwidth (especially those with high-quality factor); then a small change in the resonance frequency can reduce significantly the performance of the device. Resonant transducers have 3 main parts: excitation part (based on piezoelectric or magnetostrictive material), backing part (tail mass), and matching part (head mass) [20]. Figure 1 shows the layout of a magnetostrictive resonant transducer. Terfenol-D should be suitably magnetically and mechanically preloaded to increase the efficiency of the transducer [21]. Backing in the transducer can be a part of magnetic circuit. In design of the transducer, it is crucial to place the node of vibration exactly where prestress and bias mechanisms act in order to avoid disturbance in operation. If this condition is not guaranteed, then the efficiency of the device falls down.

2.1. Effects on Resonance Frequency. Young modulus change of Terfenol-D can change resonance frequency and mode shape. For predicting this, analytical and numerical methods

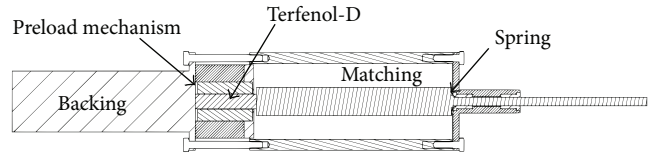

Figure 1: Layout of a magnetostrictive resonant transducer.

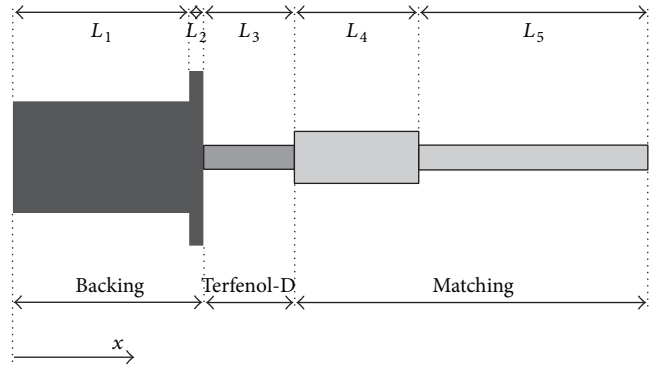

Figure 2: Main parts of the transducer.

are exploited. The vibrational behavior of the transducer can be predicted using wave equation

$$\frac{d^2u}{dx^2} + \frac{1}{A}\frac{dA}{dx}\frac{du}{dx} + \frac{\omega^2}{C^2}u = 0, \tag{1}$$

where, u is the amplitude of the vibration, A is the cross section area, ω is the circular frequency, and C is the sound speed in the material. Main parts of the transducer and coordinate system are shown in Figure 2. If main parts of the transducer are divided into 5 parts, (1) should be satisfied along them. As each part has constant cross section area, the term dA/dx is equal to zero. Thus, (1) can be reduced as

$$\frac{d^2u}{dx^2} + \frac{\omega^2}{C^2} \cdot u = 0. \tag{2}$$

General solution for (2) along the ith parts:

$$u_i = k_i \cos\left(\frac{\omega}{C_i}x\right) + k_{i+1} \sin\left(\frac{\omega}{C_i}x\right), \tag{3}$$

where k_i and k_{i+1} are constants. Diameter of each transducer part is smaller than $\lambda_i/2$ (λ_i is acoustic wavelength in each part of the transducer), to prevent lateral mode in operation [20]. Boundary conditions for solving this problem are Newton law and equivalency of displacement in interface areas of parts. Also, this transducer is free at two ends. Hence,

forces at these points are equal to zero. Equations (4) show boundary conditions for the two parts of the backing. Thus,

$$\begin{aligned} E_1 A_1 \frac{\partial u_1}{\partial x}\bigg|_{x=0} &= 0, \\ u_1(L_1) &= u_2(L_1), \\ E_1 A_1 \frac{\partial u_1}{\partial x}\bigg|_{x=L_1} - E_2 A_2 \frac{\partial u_2}{\partial x}\bigg|_{x=L_1} &= 0, \\ u_2(L_1+L_2) &= u_3(L_1+L_2), \\ E_1 A_2 \frac{\partial u_2}{\partial x}\bigg|_{x=L_1+L_2} - E_3 A_3 \frac{\partial u_3}{\partial x}\bigg|_{x=L_1+L_2} & \\ - k_{\text{screws}} u_2(L_1+L_2) &= 0. \end{aligned} \tag{4}$$

In (4), E is the Young modulus and k is stiffness. Boundary conditions for all the other parts can be easily obtained accordingly.

Considering the whole system, 10 boundary conditions can be written and resumed into

$$\overline{A} \cdot \overline{C} = \overline{0}, \tag{5}$$

where matrix $\overline{A}$ is the coefficient matrix (6), $\overline{C}$ is a row matrix of constant k_1 to k_{10} elements (8), and $\overline{0}$ is a null matrix (9).

Matrix $\overline{A}$ is then

$$\overline{A} = \begin{bmatrix} 0 & a_1 & 0 & 0 & 0 & 0 & 0 & 0 & 0 & 0 \\ b_1 & b_2 & b_3 & b_4 & 0 & 0 & 0 & 0 & 0 & 0 \\ c_1 & c_2 & c_3 & c_4 & 0 & 0 & 0 & 0 & 0 & 0 \\ 0 & 0 & d_1 & d_2 & d_3 & d_4 & 0 & 0 & 0 & 0 \\ 0 & 0 & e_1 & e_2 & e_3 & e_4 & 0 & 0 & 0 & 0 \\ 0 & 0 & 0 & 0 & f_1 & f_2 & f_3 & f_4 & 0 & 0 \\ 0 & 0 & 0 & 0 & g_1 & g_2 & g_3 & g_4 & 0 & 0 \\ 0 & 0 & 0 & 0 & 0 & 0 & h_1 & h_2 & h_3 & h_4 \\ 0 & 0 & 0 & 0 & 0 & 0 & i_1 & i_2 & i_3 & i_4 \\ 0 & 0 & 0 & 0 & 0 & 0 & 0 & 0 & j_1 & j_2 \end{bmatrix} \tag{6}$$

whose element are

$$a_1 = \frac{E_1 A_1 \omega}{C_1}, \qquad b_1 = \cos\left(\frac{\omega L_1}{C_1}\right),$$

$$b_2 = \sin\left(\frac{\omega L_1}{C_1}\right),$$

$$b_3 = -\cos\left(\frac{\omega L_1}{C_2}\right), \qquad b_4 = -\sin\left(\frac{\omega L_1}{C_2}\right),$$

$$c_1 = -a_1 b_2, \qquad c_2 = a_1 b_1,$$

$$c_3 = \frac{A_2 E_2 \omega}{C_2} \sin\left(\frac{\omega L_1}{C_2}\right), \qquad c_4 = -\frac{A_2 E_2 \omega}{C_2} \cos\left(\frac{\omega L_1}{C_2}\right),$$

$$d_1 = \cos\left(\frac{\omega(L_1+L_2)}{C_2}\right), \qquad d_2 = \sin\left(\frac{\omega(L_1+L_2)}{C_2}\right),$$

$$d_3 = -\cos\left(\frac{\omega(L_1+L_2)}{C_3}\right),$$

$$d_4 = -\sin\left(\frac{\omega(L_1+L_2)}{C_3}\right),$$

$$e_1 = -\frac{A_2 E_2 \omega}{C_2} d_2 - k_{\text{scr}} d_1, \qquad e_2 = \frac{A_2 E_2 \omega}{C_2} d_1 - k_{\text{scr}} d_2,$$

$$e_3 = -\frac{A_3 E_3 \omega}{C_3} d_4, \qquad e_4 = \frac{A_3 E_3 \omega}{C_3} d_3,$$

$$f_1 = \cos\left(\frac{\omega(L_1+L_2+L_3)}{C_3}\right),$$

$$f_2 = \sin\left(\frac{\omega(L_1+L_2+L_3)}{C_3}\right),$$

$$f_3 = -\cos\left(\frac{\omega(L_1+L_2+L_3)}{C_4}\right),$$

$$f_4 = -\sin\left(\frac{\omega(L_1+L_2+L_3)}{C_4}\right),$$

$$g_1 = -\frac{A_3 E_3 \omega}{C_3} f_2, \qquad g_2 = \frac{A_3 E_3 \omega}{C_3} f_1,$$

$$g_3 = -\frac{A_4 E_4 \omega}{C_4} f_4, \qquad g_4 = \frac{A_4 E_4 \omega}{C_4} f_3,$$

$$h_1 = \cos\left(\frac{\omega(L_1+L_2+L_3+L_4)}{C_4}\right),$$

$$h_2 = \sin\left(\frac{\omega(L_1+L_2+L_3+L_4)}{C_4}\right),$$

$$h_3 = -\cos\left(\frac{\omega(L_1+L_2+L_3+L_4)}{C_5}\right),$$

$$h_4 = -\sin\left(\frac{\omega(L_1+L_2+L_3+L_4)}{C_5}\right),$$

$$i_2 = \frac{A_4 E_4 \omega}{C_4} h_1 - k_{\text{spring}} h_2, \qquad i_3 = -\frac{A_5 E_5 \omega}{C_5} h_4,$$

$$i_4 = \frac{A_5 E_5 \omega}{C_5} h_3,$$

$$j_1 = -\frac{A_5 E_5 \omega}{C_5} \sin\left(\frac{\omega(L_1+L_2+L_3+L_4+L_5)}{C_5}\right),$$

$$j_2 = \frac{A_5 E_5 \omega}{C_5} \cos\left(\frac{\omega(L_1+L_2+L_3+L_4+L_5)}{C_5}\right). \tag{7}$$

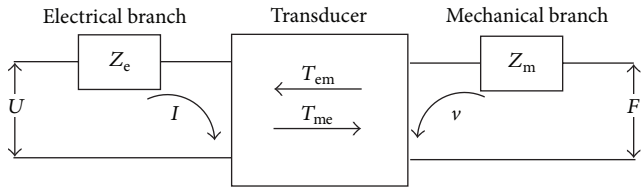

Figure 3: Model of ideal gyrator.

Matrix $\overline{C}$ is

$$\overline{C} = \begin{bmatrix} k_1 & k_2 & k_3 & k_4 & k_5 & k_6 & k_7 & k_8 & k_9 & k_{10} \end{bmatrix}^T. \quad (8)$$

As it is known, necessary condition for the solution existence of (5) is

$$\det\left(\overline{A}\right) = 0. \quad (9)$$

Roots of (9) are longitudinal resonance frequencies. Thus, resonance frequencies are function of each parameter of matrix $\overline{A}$, including Young modulus of Terfenol-D (E_3). This relationship allows considering the effect of a change in the Young modulus of the material on the behavior of the device.

Analytical model is supported by a finite element model of the device. ANSYS12 commercial software has been used to carry out modal simulation to predict resonance frequency and mode shape of the transducer.

2.2. Effects on Quality Factor. A magnetostrictive transducer can be modeled with ideal gyrator as shown in Figure 3 [4]. Equations of this gyrator are presented in (10a) and (10b) [14]:

$$U = Z_e \cdot I + T_{em} \cdot v, \quad (10a)$$

$$F = T_{me} \cdot I + Z_m \cdot v, \quad (10b)$$

where U is the applied voltage, I is the current, and F and v are mechanical force and speed, respectively. T_{em} is the electromotive force per velocity and T_{me} is the mechanical force per current. In free state condition of the transducer, there is no mechanical force. By setting $F = 0$ in (10a) and substituting the result in (10b), effective electrical impedance of the transducer Z_{ee} can be calculated. This parameter is presented in [20]

$$Z_{ee} = R_{ee} + j \cdot x_{ee} = Z_e + \frac{-T_{me} \cdot T_{em}}{Z_m} = Z_e + Z_{mot}, \quad (11)$$

where R_{ee} and x_{ee} are real and imaginary parts of the transducer impedance, Z_e is the electrical impedance, and Z_{mot} is motional impedance. If Z_{ee} is measured in clamped state, Z_{mot} is vanished. Thus, Z_{mot} can be obtained by measuring impedance in free and clamped state condition.

Real and imaginary parts of Z_{mot} form a circle in resonance region frequency. This circle is tangent to origin. For presented transducer, this circle is depicted in Figure 4. If the diameter between origin and the points of circle that corresponds to resonance frequency is drawn, perpendicular line to this diameter crosses the circle at two points. These

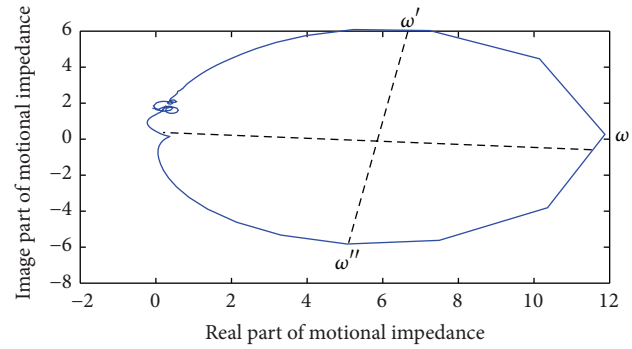

Figure 4: Motional impedance locus.

Figure 5: The transducer used for tests.

points correspond to ω' and ω''. $\omega'' - \omega'$ show bandwidth of the transducer [20]. Thus, quality factor can be calculated using (12) [22]. In the following equation, ω_0 is the circular resonance frequency:

$$Q_m = \frac{\omega_0}{\omega'' - \omega'}. \quad (12)$$

3. Experimental Validation

3.1. The Resonant Transducer. To experimentally investigate ΔE effect, resonant magnetostrictive transducers have been tested under different operating condition (Figure 5). The transducer has been designed for working in the second mode (Figure 6). Resonance frequency for this transducer is 8252 Hz. Magnetic bias in the presented transducer is 40 kA/m and mechanical prestress is 10.34 MPa. Magnetic bias has been supplied by ceramic permanent magnet and prestress has been exerted by 4 screws and a bevel spring. Magnetic yoke was used to close magnetic flux path and minimize flux leakage. Excitation coil has 1000 turns of wire with 1 mm^2 cross section area. In designing the transducer, prestress and bias mechanisms are attached to nodes of vibration in order to avoid disturbance in operation (Figure 6). Table 1 shows main dimensions of the device.

3.2. ΔE Effect Measurement. There are some methods for Young modulus measurement. Stress-Strain graph, acoustic

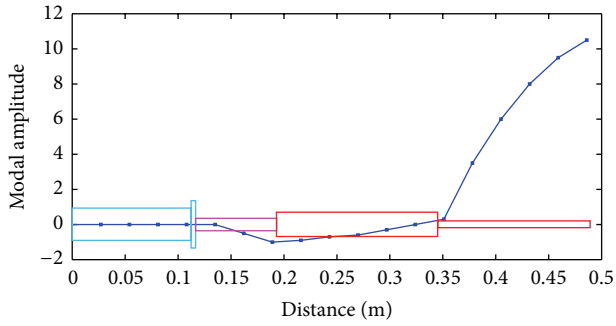

Figure 6: Modal shape of the transducer obtained with ANSYS12.

Table 1: Transducer main dimensions.

Main part	Length [mm]	Diameter [mm]
Backing	150	50
Terfenol-D	50	10
Matching	157.5	23
	157.5	7

and impedance methods are the most important. Stress-Strain graph has some intrinsic error such as data pickup. High attenuation of transverse wave in Terfenol-D makes some problem for acoustic measurement. Thus, impedance method has been selected. For using impedance method, a search coil is turned to Terfenol-D. Resonance frequency of Terfenol-D can be detected with measurement impedance of the coil. In resonance band of frequency, there is unusual change in impedance response. If constant voltage mode of impedance analyzer was used, the maximum pick in this region would be resonance frequency and minimum pick would be antiresonance frequency [20]. Young modulus can be calculated by

$$E = 2\pi\rho f_{\text{res}} l^2. \tag{13}$$

3.3. Experimental Set-Up. First tests for ΔE effect measurement have been done on the magnetostrictive rod. Experimental set-up is shown in Figure 7. The Terfenol-D rod is wounded by an excitation coil to change the magnetic field and it is surrounded by a search coil. The search coil is connected to the impedance analyzer. To minimize flux leakage, a high permeability yoke made of pure iron has been considered in the set-up.

Tests have been carried out changing the magnetic bias and the mechanical prestress of Terfenol-D. The change in the first is obtained exploiting the excitation coil of the set-up. Preload of the magnetostrictive rod can be easily modified by means of 4 screws and can be measured using a load cell. Necessary calibration with standard weights has been done. A temperature control circuit was used to keep temperature of Terfenol-D constant during the test. By using this set-up, effect of the mentioned parameter in Terfenol-D Young modulus was measured precisely. Results of measurements would be input for FEM and analytical methods to predict mode shape and resonance frequency.

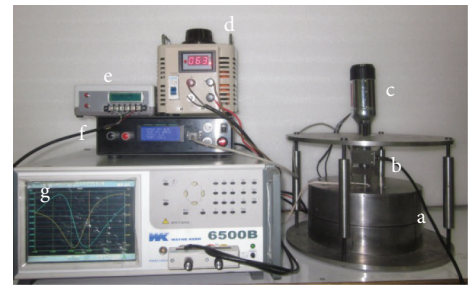

Figure 7: The experimental set-up for measurement of Young modulus ((a) magnetic yoke, (b) load cell, (c) heater, (d) power supply, (e) load indicator, (f) temperature control unit, and (g) impedance analyzer).

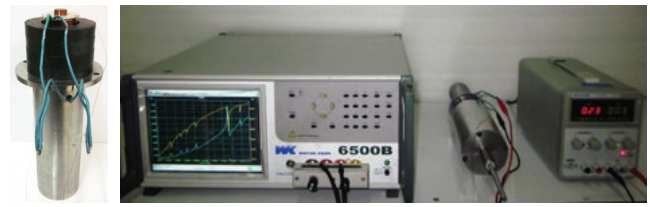

Figure 8: Experimental set-up for measuring changes in resonance frequency.

Supplementary tests are carried out to verify analytical and numerical resonance frequency prediction. The experimental set-up for these tests is shown in Figure 8. A search coil is attached to impedance analyzer; excitation coil of transducer is used as bias coil. Mechanical preloading is exerted by screws and can be adjusted by a torque meter. With using this set-up, effect of change in magnetic bias and prestress on resonance frequency of the transducer can be experimentally studied. Moreover, according to (11), quality factor can be calculated.

4. Results and Discussion

Figure 9 shows the relationship between the Young modulus of Terfenol-D rod and magnetic bias in different prestress levels. The temperature was kept at 20°C. Range of magnetic field in this figure is from 20 kA/m to 100 kA/m. These values for prestress and magnetic field are common for Terfenol-D transducers. According to this figure, Young modulus changed between 40 and 75 GPa. Figure 10 depicts dependency of Young modulus on temperature in 40 kA/m bias and 10.34 MPa prestress. By changing temperature between 20°C and 80°C, Young modulus is changed about 5 MPa.

By applying ΔE effect to analytical and FEM model, resonance frequency and mode shape have been calculated. Figures 11, 12, and 13 show effects of magnetic bias and mechanical prestress on the transducer resonance frequency obtained from FEM and analytical method. Results show that, in the transducer with the mentioned design, the effect of Young modulus can change the resonance frequency about 220 Hz. As this kind of device has a very narrow bandwidth, a similar change in resonance frequency considerably reduces

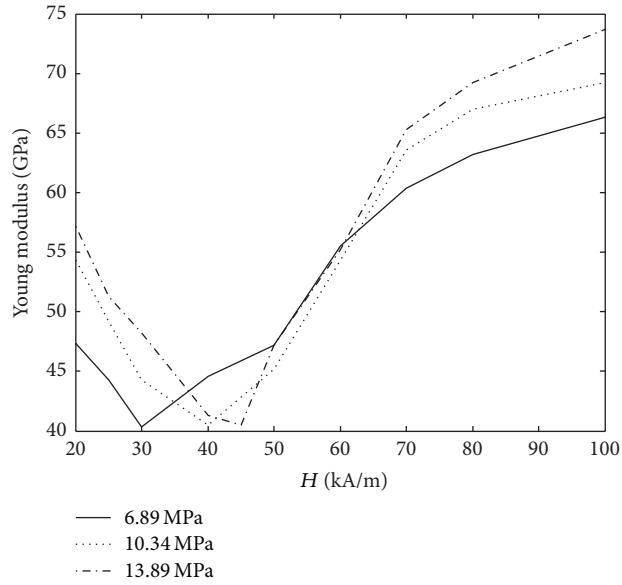

Figure 9: Young modulus versus magnetic bias field in different prestress level in 20°C.

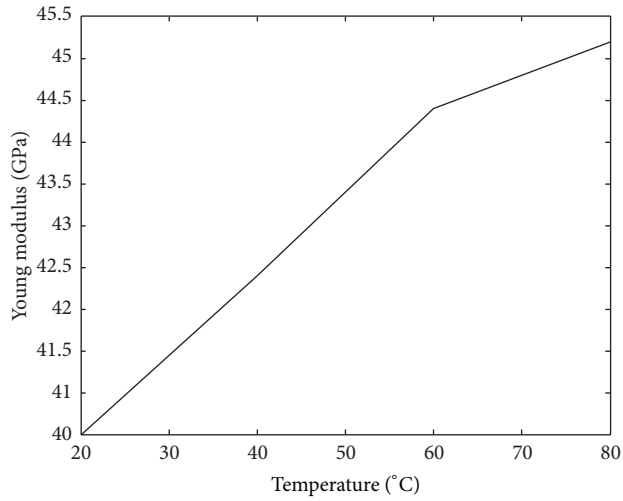

Figure 10: Young modulus versus temperature in 10.34 MPa prestress and 40 kA/m magnetic bias field.

the efficiency of the transducer. This effect is more conspicuous for high-quality factor transducer.

Table 2 shows effect of temperature on resonance frequency obtained from FEM and analytical method. In both methods, effect of temperature until 80°C is less than 15 Hz.

Figure 14 shows effect of Young modulus change on mode shape. Node location is extremely important as they have to correspond to places where both the spring and the preloading mechanisms act. A change in the position of the node corresponds to a disturbance on the ideal working condition of the device. Figure 15 shows changing first and second node location in different Young modulus. In the presented transducer, maximum changing for node locations is about 8 mm.

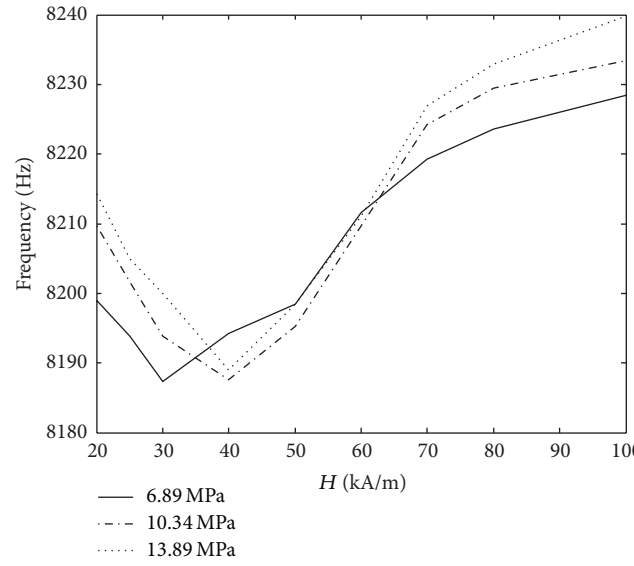

Figure 11: Analytical prediction of resonance frequency in different magnetic bias in 13.89 MPa prestress.

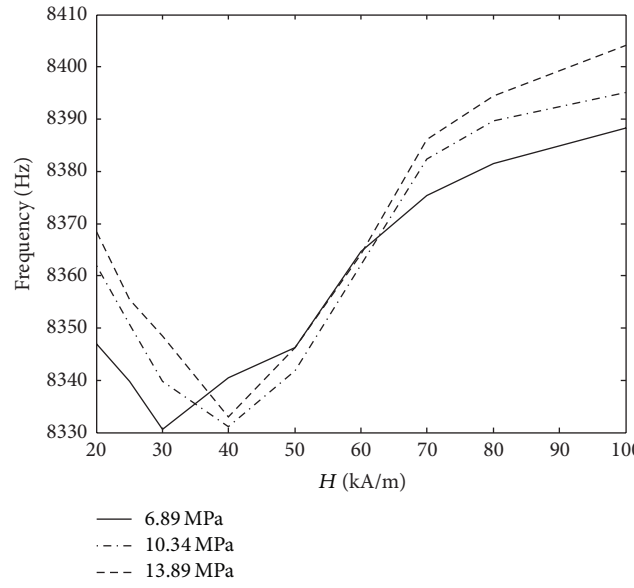

Figure 12: FEM prediction of resonance frequency in different magnetic bias in 13.89 MPa prestress.

Table 2: Resonance frequency in different temperature (10.34 MPa prestress, 40 kA/m magnetic bias).

T (°C)	Young modulus (GPa)	FEM prediction of resonance frequency (Hz)	Analytical prediction of resonance frequency (Hz)
20	40.5	8188	8331
40	42.4	8191	8335
60	44.4	8194	8340
80	45.2	8195	8342

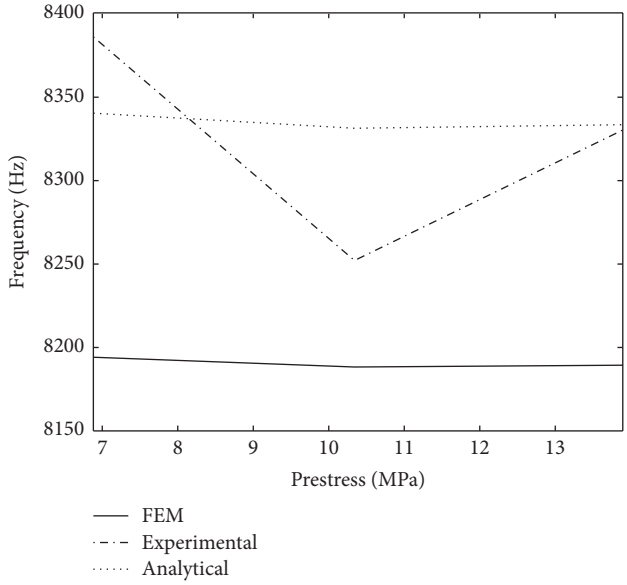

Figure 13: Resonance frequency in different prestress in 40 kA/m magnetic bias.

For experimental verification and calculating quality factor, impedance response of the transducer in different magnetic bias has been studied. Figure 16 shows impedance response of the transducer in different magnetic bias field.

Table 3 shows experimental verification of FEM and analytical prediction for resonance frequency. Good agreement can be seen with near 97% accuracy. It happened because precise material properties are applied in both analytical and FEM methods. In Table 3, effect of changing in magnetic bias on mechanical quality factor has been also reported. In range of application, mechanical quality factor varies much with magnetic bias. It can happen from changing node locations and also variation in Terfenol-D damping coefficient. Because of changing node locations, a part of the transducer energy is consumed for vibrating high stiffness prestress mechanism. Changing quality factor reduces vibration amplitude of the transducer.

5. Conclusions

In this paper, ΔE effect and its influence on vibrational behavior of the Terfenol-D transducer have been studied. First the effect of Young modulus change on resonance frequency and mode shape was studied through both analytical and numerical methods. Experimental tests on Terfenol-D have allowed measuring ΔE effect in different operating conditions. Then, a resonant transducer has been tested to validate analytical and numerical predictions. Results of both methods for resonance frequency were verified with experiment in different operational condition. In addition, effect of changing operational condition on quality factor was studied experimentally.

Results show that, with this type of transducer, ΔE effect leads to a change in the resonance frequency about 4 percent.

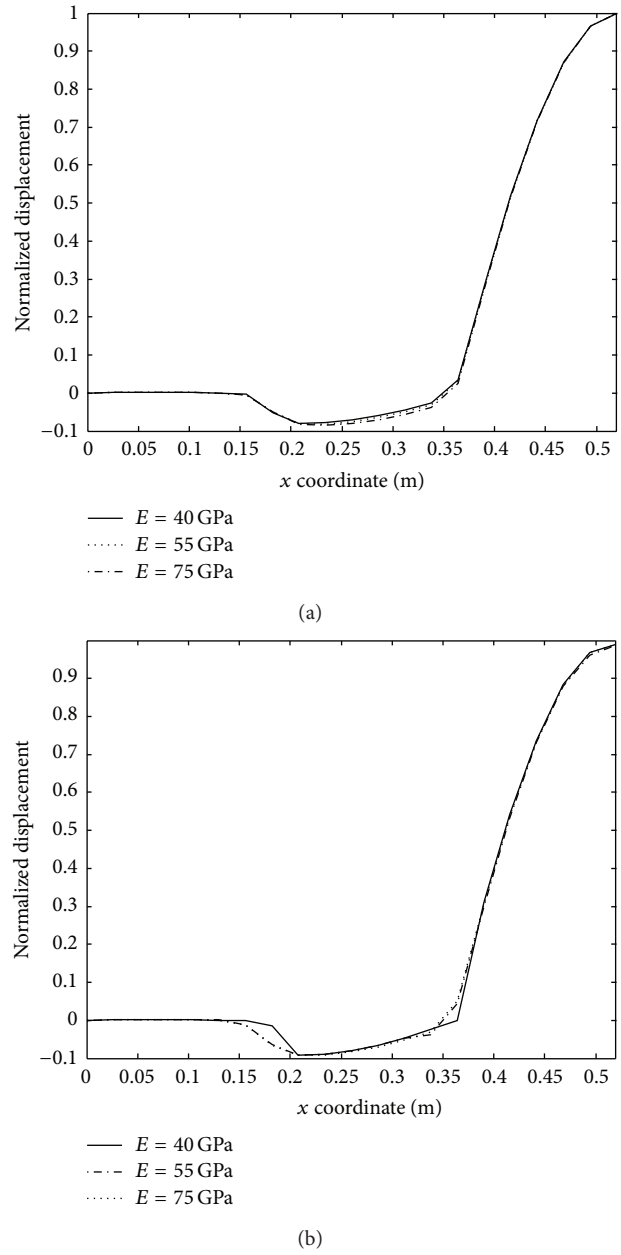

Figure 14: Mode shape in different Young modulus: (a) FEM simulation, (b) analytical method.

Even if this change can be considered as small, as the bandwidth of the transducer is very narrow, the performance of the device can be affected negatively if this effect is neglected. Furthermore, quality factor of this transducer considerably changes and it can reduce the efficiency of the transducer. As a matter of fact, quality factor falls down from 112.1 to 33.92.

Changes in mode shape strongly affect the performance of the device. As bias mechanism of the transducer has been designed to be attached on nodes of vibration, the displacement of a node leads to a loss of isolation between them and main parts of the transducer and energy cannot be transmitted efficiently. Also, the transducer is fixed through nodes and changing node locations interferes in operation.

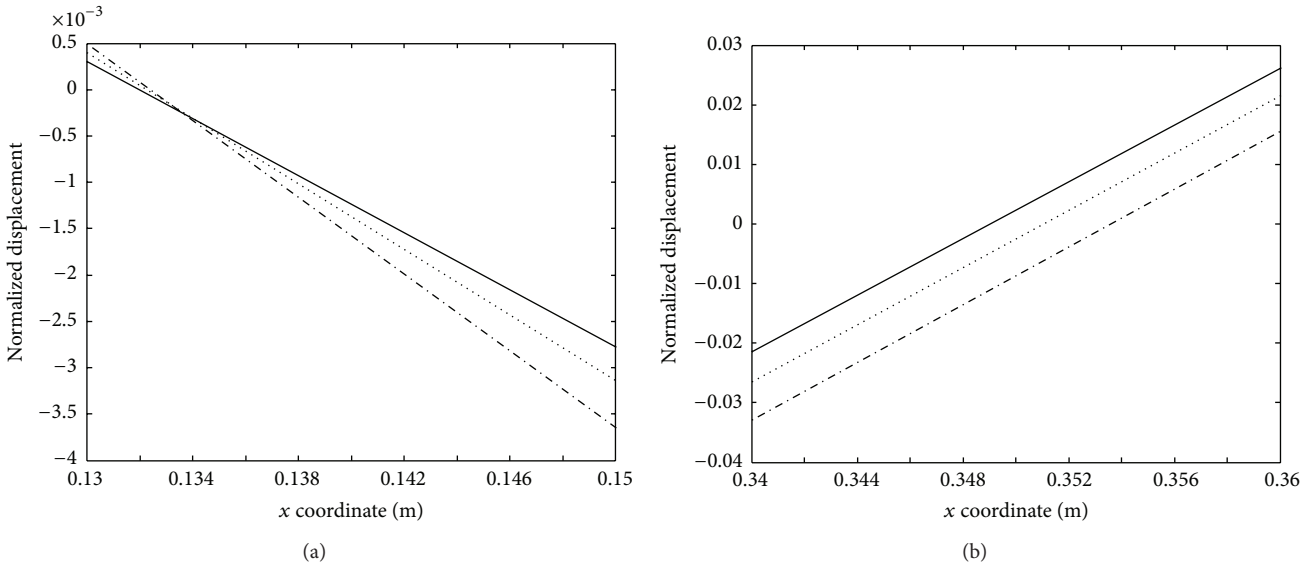

Figure 15: FEM prediction for changing node location in different Young modulus: (a) first node, (b) second node.

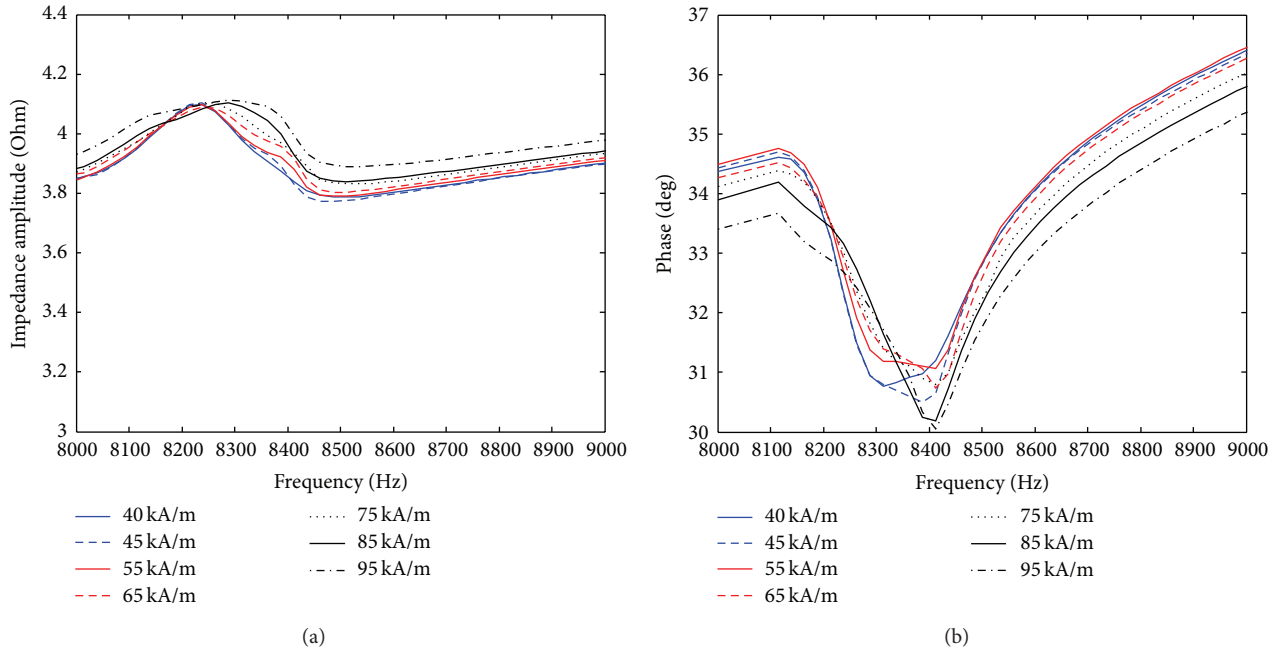

Figure 16: (a) Amplitude and (b) phase of the transducer in different magnetic bias in 13.89 MPa.

Table 3: Experimental verification in 13.89 MPa prestress.

H (kA/m)	Young modulus (GPa)	FEM prediction of resonance frequency (Hz)	Analytical prediction of resonance frequency (Hz)	Experimental resonance frequency (Hz)	Q
40	41.3	8189	8342	8330	57
45	40.5	8188	8331	8325	112.71
55	51.7	8206	8356	8350	82.80
65	60.6	8220	8376	8387	42.14
75	67.6	8230	8391	8405	40.02
85	70.7	8235	8398	8410	37.39
95	73.7	8240	8403	8414	33.92

Conflict of Interests

The authors declare that there is no conflict of interests regarding the publication of this paper.

References

[1] A. E. Clark, *Ferromagnetic Materials*, vol. 1, North Holland, Amsterdam, The Netherlands, 1980.

[2] A. Grunwald and A. G. Olabi, "Design of a magnetostrictive (MS) actuator," *Sensors and Actuators: A Physical*, vol. 144, no. 1, pp. 161–175, 2008.

[3] J. L. Pons, *Emerging Actuator Technologies: A Micromechanical Approach*, 2005.

[4] G. Engdahl, Ed., *Handbook of Giant Magnetostrictive Materials*, Royal Institute of Technology, Stockholm, Sweden, 2000.

[5] F. Braghin, S. Cinquemani, and F. Resta, "A low frequency magnetostrictive inertial actuator for vibration control," *Sensors and Actuators A: Physical*, vol. 180, pp. 67–74, 2012.

[6] C. May, K. Kuhnen, P. Pagliaruolo, and H. Janocha, "Magnetostrictive dynamic vibration absorber (DVA) for passive and active damping," in *Proceedings of the Euronoise*, Naples, Italy, 2003.

[7] T. Zhang, C. Jiang, H. Zhang, and H. Xu, "Giant magnetostrictive actuators for active vibration control," *Smart Materials and Structures*, vol. 13, no. 3, pp. 473–477, 2004.

[8] F. Braghin, F. Castelli-Dezza, S. Cinqueman, and F. Resta, "A full-range hybrid device for sound reproduction," *Smart Structures and Systems*, vol. 11, no. 6, pp. 605–621, 2013.

[9] S. Deras and C. Yuk, "Underwater sonar transducer using magnetostrictive material," *Journal of Magnetics*, vol. 4, no. 3, pp. 98–101, 1994.

[10] K. R. Dhilsha, G. Markandeyulu, B. V. P. Subrahmanyeswara Rao, and K. V. S. Rama Rao, "Design and fabrication of a low frequency giant magnetostrictive transducer," *Journal of Alloys and Compounds*, vol. 258, no. 1-2, pp. 53–55, 1997.

[11] A. I. Markov, *Ultrasonic Machining of Intractable Materials*, Iliffe Books, London, UK, 1966.

[12] A. G. Olabi and A. Grunwald, "Design and application of magnetostrictive materials," *Materials & Design*, vol. 29, no. 2, pp. 469–483, 2008.

[13] H. T. Savage, A. E. Clark, and D. Pearson, "The stress dependence of the ΔE effect in Terfenol–D," *Journal of Applied Physics*, vol. 64, no. 10, p. 5426, 1988.

[14] Y. Liang and X. Zheng, "Experimental researches on magneto-thermo-mechanical characterization of Terfenol-D," *Acta Mechanica Solida Sinica*, vol. 20, no. 4, pp. 283–288, 2007.

[15] R. Kellogg and A. Flatau, "Experimental investigation of terfenol-D's elastic modulus," *Journal of Intelligent Material Systems and Structures*, vol. 19, no. 5, pp. 583–595, 2008.

[16] R. Kellogg and A. Flatau, "Wide band tunable mechanical resonator employing the $\triangle$E effect of Terfenol-D," *Journal of Intelligent Material Systems and Structures*, vol. 15, no. 5, pp. 355–368, 2004.

[17] Y. Yong and L. Lin, "Dynamic model considering the ΔE effect for giant magnetostrictive actuators," in *Proceedings of the IEEE International Conference on Control and Automation*, pp. 667–672, Christchurch, New Zealand, December 2009.

[18] T. Ueno, J. Qiu, and J. Tani, "Magnetic circuit design method for magnetic force control systems using inverse magnetosrtictive effect: examination of energy conversation efficiency depending on ΔE effect," *Electrical Engineering in Japan*, vol. 140, no. 1, pp. 8–15, 2002.

[19] M. J. Dapino, R. C. Smith, and A. B. Flatau, "Model for the delta-E effect in magnetostrictive transducers," in *Smart Structures and Materials 2000: Smart Structures and Integrated Systems*, vol. 3985 of *Proceedings of SPIE*, June 2000.

[20] A. Abdullah, M. Shahini, and A. Pak, "An approach to design a high power piezoelectric ultrasonic transducer," *Journal of Electroceramics*, vol. 22, no. 4, pp. 369–382, 2009.

[21] R. Frederick, *Ultrasonic Engineering*, Wiley, New York, NY, USA, 1965.

[22] G. Mojtaba, U. Toshiyuki, and M. Mehdi, "Quality factor, static and dynamic responses of miniature galfenol actuator at wide range of temperature," *International Journal of Physical Sciences*, vol. 6, no. 36, pp. 8143–8150, 2010.